Proceedings of the 4th Jagiellonian Symposium on Advances in Particle Physics and Medicine

Alpha and Cluster Decay in r-Process Nucleosynthesis

N.G. Kelkar[a,*], D.F. Rojas-Gamboa[a], O.L. Caballero[b] and J.E. Perez Velasquez[c]

[a] *Departamento de Fisica, Universidad de los Andes, Carrera 1E No. 18A-10, 111711, Bogotá, Colombia*
[b] *Department of Physics, University of Guelph, N1G 2W1, Guelph, ON, Canada*
[c] *Facultad del Medio Ambiente y Recursos Naturales, Universidad Distrital Francisco José de Caldas, Calle 13, No. 31-75, 111611, Bogotá, Colombia*

Doi: 10.12693/APhysPolA.142.324 *e-mail: nkelkar@uniandes.edu.co

Elements from iron to uranium are expected to have been produced in the r-process nucleosynthesis via rapid neutron capture at elevated temperatures of the order of Giga Kelvins (GK). The network of coupled differential equations used to determine the abundance of elements thus involves nuclear reaction rates at elevated temperatures. The path of the r-process nucleosynthesis is along highly unstable nuclei and hence nuclear decay rates play an important role too. However, standard codes available for such calculations make use of terrestrial half-lives for alpha decay. Within a statistical approach and using data on excited nuclei, we find that for temperatures between 1–2 GK, the alpha decay half-lives can decrease by a few orders of magnitude as compared to the terrestrial ones. Based on these results, an estimate for the variations of the abundance of elements due to temperature-dependent half-lives is provided for a high entropy wind scenario. A model for the radioactive decay of thermally excited heavy nuclei by emitting an alpha or a light cluster such as ^{14}C, ^{20}O, or ^{28}Mg is also presented and applied to evaluate the less known light cluster decay rates.

topics: alpha decay, cluster decay, r-process nucleosynthesis

1. Introduction

Synthesis of elements and the underlying nuclear physics has been a field at the frontiers of physics for several decades. With the exception of a few anomalies, such as the lithium problem [1] in big bang nucleosynthesis, one can say that we have a fairly good understanding of the mechanism and production sites of the light and medium-heavy elements. "How were the elements from iron to uranium made?", however, remains a question to be answered in the next decade [2]. The general conditions required to cook these heavy elements seem to be clear, but the sites and means of production are not very well understood. It seems difficult to form nuclei beyond iron by fusion since the transmission through the Coulomb barrier decreases drastically with increasing nuclear charges, making fusion impossible for large nucleon numbers. Neutron-induced reactions then emerge as the mechanism for the synthesis of the heavy nuclides due to the absence of the Coulomb barrier and the occurrence of large neutron capture cross sections. Thus, it seems that heavy nuclides can be synthesized by exposing lighter seed nuclei to a source of neutrons.

The r-process, which occurs along a path close to the neutron drip line in the nuclear landscape, provides the mechanism for the origin of more than half of the heavy nuclei in the universe [3, 4]. Candidates for the possible sites of r-process nucleosynthesis are several, with neutrino winds from core-collapse supernovae and neutron star mergers being among them [5]. In addition to producing kilohertz gravitational waves detectable by ground-based interferometers, compact object mergers involving a neutron star are likely to emit a variety of electromagnetic signals. The mergers may also produce optical/infrared transients powered by the radioactive decay of heavy elements synthesized via rapid neutron capture (the r-process).

The r-process nucleosynthesis path, in general, is along very unstable and neutron-rich nuclei. The explosive conditions in r-process sites could result in nuclei existing in excited states since the population factor for excited energy levels of a nucleus is large at high ambient temperatures. Calculation of nuclear abundances, in general, requires the evolution of nuclear abundances via a nuclear reaction network made up of a system of the first order (coupled) differential equations with production

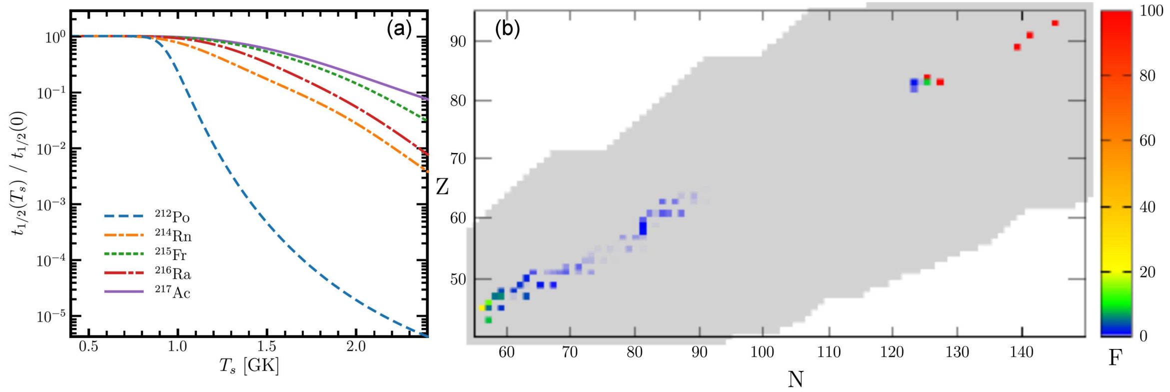

Fig. 1. Temperature dependence of the alpha decay half-lives is shown in panel (a). Panel (b) shows the sensitivity factor (4) of the abundance of elements due to the change in alpha decay half-lives (see text for details).

and destruction terms involving each of the many nuclear reactions and decays involved [5]. The possible effects of the nuclear thermal excitations are taken into account in the forward and reverse reaction rates. However, the same is not true in the case of alpha decays. The latter are taken from measured half-lives on earth. In this work, we investigate the changes in the alpha decay half-lives at elevated temperatures using experimental information on the excited levels of nuclei. Apart from this, the cluster decay mode, which is usually considered unimportant due to its low branching fraction as compared to other decay modes (such as alpha decay and fission) and not included in the r-process nucleosynthesis codes, is also investigated at high temperatures. In the absence of sufficient experimental data, we propose a temperature-dependent double folding model for such a calculation. An estimate for the variations of the abundances due to changes in the alpha decay rates at high temperatures presented here provides the motivation for a detailed investigation of the same in the future.

2. Half-lives at elevated temperatures

The temperature-dependent half-life, $t_{1/2}(T_s) = \ln(2)/\lambda(T_s)$, is evaluated using the standard formula for the temperature-dependent decay constant [6, 7], namely,

$$\lambda(T_s) = \sum_i p_i \sum_j \lambda_{ij}. \tag{1}$$

Here, the sums over i and j are over the parent and daughter states, respectively. Thus, λ_{ij} is the decay constant for the decay of the i-th level in the parent to the j-th level in the daughter. The population probability, p_i, is given with a Boltzmann factor as [7]

$$p_i = \frac{(2J_i+1)\,\mathrm{e}^{-E_i/(k_\mathrm{B}T_s)}}{\sum_l (2J_l+1)\,\mathrm{e}^{-E_l/(k_\mathrm{B}T_s)}}, \tag{2}$$

where J_i and E_i are the spin and the excitation energy of the state i, respectively. Inserting (2) in (1),

$$\lambda(T_s) = \frac{\ln(2)}{\sum_l (2J_l+1)\,\mathrm{e}^{-E_l/(k_\mathrm{B}T_s)}} \times \sum_{i,j} \frac{(2J_i+1)}{t^i_{1/2}}\,\mathrm{e}^{-E_i/(k_\mathrm{B}T_s)}\,(BR)_{ij}, \tag{3}$$

where $(BR)_{ij}$ is the branching fraction for the decay from the i-th level of the parent nucleus to the j-th level in the daughter nucleus. The detailed decay schemes and the percentage decay to a particular channel, i.e., $I = (\lambda_{ij}/\lambda_\mathrm{tot}) \times 100\%$ can be found on the website [8]. The branching fraction, $(BR)_{ij} = \lambda_{ij}/\lambda_\mathrm{tot}$, can thus be obtained from the data tables.

2.1. Thermally enhanced alpha decay rates

Using (3) with the input half-lives, $t^i_{1/2}$ and $(BR)_{ij}$ taken from experiment, in general, leads to a decrease in the temperature dependent half-life, $t_{1/2}(T_s)$ of a given nucleus. For those levels with unknown experimental half-lives, a universal decay law [9] with an effective Q-value, $Q_\mathrm{eff} = Q + \bar{\epsilon}(A,Z,T_s)$, (where $\bar{\epsilon}(A,Z,T_s)$ is obtained using the standard definition of the average excitation energy [10] in statistical physics) is used to estimate $t^i_{1/2}$ of those levels. Half-lives of the nuclei, ^{212}Po, ^{214}Rn, ^{215}Fr, ^{216}Ra, and ^{217}Ac, are presented in Fig. 1a as a function of the ambient temperature, T_s. The choice of these nuclei, which have the neutron number $N = 128$, was based on the findings in [11] where it was observed that the nuclei with $N = 128$ had the highest decay rates. In terms of a preformed cluster model with an alpha tunneling the Coulomb barrier formed by its interaction with the daughter, this implied that the alpha spends the least amount of time with the daughter with $N = 126$ at the shell closure. Not surprisingly, these nuclei have a good number of excited levels decaying by alpha decay as compared to other nuclei. Figure 1a shows that the half-lives decrease by about 1–2 orders of magnitude in most cases as compared to the terrestrial half-lives, except for the case of ^{212}Po where the decrease is about 5 orders of magnitude. The possible reason for this large decrease could simply be the large number of excited states of ^{212}Po as compared to other nuclei. We note that the daughter nucleus, ^{208}Pb in this case is doubly magic.

To estimate the effect of thermally enhanced alpha decay rates on the r-process yields, we performed a sensitivity calculation with the sensitivity module of SiRop (available at [12]). SiRop is an updated version of r-Java [13, 14], that allows for handling nuclear physics inputs, setting up different astrophysical conditions, and customize sensitivity factor metrics [15] for nucleosynthesis studies. For the astrophysical environment we chose a high entropy wind site. The initial seed abundances were determined by nuclear statistical equilibrium at a temperature of 3 GK, a density of 8×10^{11} g/cm^3, and an initial electron fraction $Y_{e,o} = 0.2$. The entropy of the wind is $S = 200$ in units of k_{B}/baryon. These conditions produced r-process elements beyond the third peak at mass number $A = 195$, allowing us to study the effect of alpha decay.

Motivated by the changes found in the half-lives, we multiplied the alpha decay rates by a factor of 100 for all $Z \geq 82$ nuclei. Although we have found that for some nuclides, alpha decay rates can be enhanced by a greater factor, even orders of magnitude as in ^{212}Po, we keep these conservative changes. To assess the effect of changing the α-decay rates on the abundances, we use as a metric the factor

$$F = \frac{|Y - Y_{\mathrm{base}}|}{Y_{\mathrm{base}}}, \tag{4}$$

with Y_{base} being the baseline abundance. Figure 1b shows the sensitivity factor F (color scale) when the alpha decay rate is increased by a factor of a hundred, as described above. One can see that some of the abundances of some of the stable heavy nuclei are affected by changing the alpha decay rates.

Although the impact is, in most cases, modest, keeping in mind that we altered the half-lives of a small set of nuclei, the results motivate further studies. We are mindful that not all half-lives will decrease by the same factor. Also, we expect that the impact will be different in other astrophysical scenarios. However, as long as alpha emitters get produced, there is a potential impact of the thermally enhanced alpha decay rates on the r-process element abundances evolution, which we will explore in future work.

2.2. Model for cluster decay at elevated temperatures

Cluster radioactivity [16, 17], which involves the decay of a heavy parent nucleus into a light cluster such as ^{14}C, ^{20}O, ^{24}Ne, etc., and a heavy daughter nucleus, is usually not considered important due to its low branching ratio as compared to alpha decay and is hence not included in r-process nucleosynthesis calculations. However, considering the significant sensitivity of alpha decay half-lives to the ambient temperature, it seems worth investigating the same in cluster decay. In case the cluster decay rates are more strongly enhanced due to temperature, this decay mode may play a competing role with alpha decay at high temperatures.

In the absence of sufficient information on the cluster decay rates of excited nuclei to daughters in their ground or excited states, we propose a theoretical model in order to estimate the change in decay rates with the temperature of the surrounding. It is based on a double folding model (DFM), which has been shown in our earlier works [18, 19] to be quite successful in reproducing the available alpha and cluster decay rates measured on earth. We extend it within reasonable theoretical assumptions to calculate the half-lives of excited parent nuclei decaying to the ground and the excited states of the daughter nuclei. The latter exercise is carried out by relating the excitation energy of the nucleus to a "nuclear temperature" and formulating a DFM with temperature-dependent nuclear densities. The excitation energy of the parent nucleus is incorporated through an effective Q value, which reflects a shift in the energy of the tunneling light cluster which is taken to be in its ground state.

Within a semiclassical framework, the spontaneous emission of a charged particle (or light nucleus) can be described as a quantum tunneling phenomenon of the particle through the Coulomb barrier. This requires the assumption of a preformed cluster of the emitted nuclei inside the parent nucleus. Using the Jeffreys–Wentzel–Kramers–Brillouin (JWKB) approximation [20], different semiclassical approaches lead to the same expression for the decay width [21], $\Gamma = \hbar \ln(2)/t_{1/2}$. In order to extend the cluster decay half-life calculations to excited states, the excitation energy relative to the ground state is included in both the energy of the emitted cluster and the interaction potential. Therefore, the energy of the cluster is taken as an effective Q value given by $Q_{\mathrm{eff}} \equiv Q + E_p^* - E_d^* = Q + \Delta E^*$, where E_p^* and E_d^* are the excitation energies of the parent and daughter nuclei, respectively, and ΔE^* is the difference between them.

The nuclear potential is calculated using a realistic nucleon–nucleon (NN) interaction folded with the density distributions of both interacting nuclei (i.e., the heavy daughter and the light cluster which are preformed in the parent) [11, 21]. The excitation energy effects are included via the nuclear density distributions defining a nuclear temperature T of the daughter nucleus as [22] $E_d^*(T) = \frac{1}{9} A T^2$. The temperature-dependent matter density distribution, $\rho_d(r; E_d^*(T))$, of the excited daughter nucleus is given as in [23, 24].

The nuclear potential is then obtained within the double-folding model [25] as

$$V_{\mathrm{N}}\big(\boldsymbol{r};E_d^*(T)\big) = \int \mathrm{d}\boldsymbol{r}_c \int \mathrm{d}\boldsymbol{r}_d\, \rho_c\left(\boldsymbol{r}_c\right) v_{\mathrm{N}}\big(|\boldsymbol{s}| = |\boldsymbol{r}+\boldsymbol{r}_c-\boldsymbol{r}_d|\big)\, \rho_d\left(\boldsymbol{r}_d;E_d^*(T)\right), \tag{5}$$

where the effective NN interaction based on the M3Y-Reid-type soft core potential is used [25].

The excitation energy-dependent Coulomb potential is evaluated in a similar manner by using the T-dependent charge density distributions normalized to the atomic number Z. Thus, the total potential is given by

$$V\left(r;E_p^*,E_d^*\right) = \lambda\left(E_p^*,E_d^*\right) V_{\mathrm{N}}\left(r;E_d^*\right) + V_{\mathrm{C}}\left(r;E_d^*\right) + \frac{\hbar^2}{2\mu\, r^2}\left(l+\tfrac{1}{2}\right)^2 . \tag{6}$$

where r is the separation between the center of masses of the cluster and the daughter nucleus. Note that the usual centrifugal barrier has been replaced by the Langer modified one [26] since the width is evaluated within a semiclassical approximation. The strength of the nuclear interaction, $\lambda\left(E_p^*,E_d^*\right)$, is fixed by imposing the Bohr–Sommerfeld quantization condition. This also determines the depth of the nuclear potential for different excited states of the parent and daughter nuclei as

$$\int\limits_{r_1(E_p^*,E_d^*)}^{r_2(E_p^*,E_d^*)} \mathrm{d}r\, k\left(r;E_p^*,E_d^*\right) = \frac{\pi}{2}(G-l+1), \tag{7}$$

where $k(r;E_p^*,E_d^*) = \sqrt{\frac{2\mu}{\hbar^2}\left|V(r;E_p^*,E_d^*)-Q_{\mathrm{eff}}\right|}$ is the wave number. The turning points, r_i, depend parametrically on the excited states through the condition $V\left(r_i;E_p^*,E_d^*\right) = Q_{\mathrm{eff}}$, and n is the number of nodes of the quasibound wave function of the light cluster-daughter nucleus relative motion. This is expressed as $n = \frac{1}{2}(G-l)$, where G is a global quantum number, and l is the relative orbital angular momentum quantum number (see [19] for details).

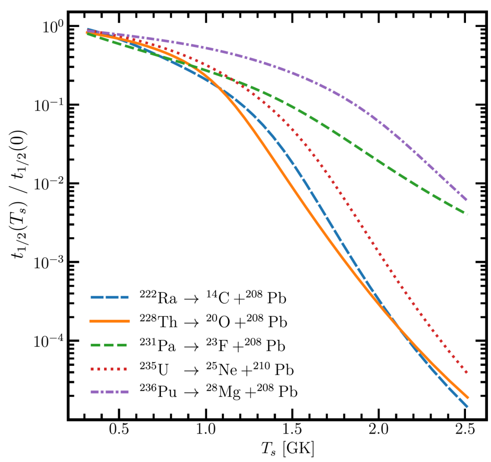

Fig. 2. Temperature dependence of the cluster decay half-lives.

We can now write the decay width for an excitation energy-dependent double folding model within the semiclassical JWKB approximation as

$$\Gamma\left(E_p^*,E_d^*\right) = P_c\,\frac{\hbar^2}{2\mu}\left[\int\limits_{r_1(E_p^*,E_d^*)}^{r_2(E_p^*,E_d^*)} \frac{\mathrm{d}r}{k\left(r;E_p^*,E_d^*\right)}\right]^{-1} \times \exp\left(-2\int_{r_1(E_p^*,E_d^*)}^{r_2(E_p^*,E_d^*)} \mathrm{d}r\, k\left(r;E_p^*,E_d^*\right)\right), \tag{8}$$

with P_c being the cluster preformation probability. The excitation energy-dependent half-life is then calculated as [27]

$$t_{1/2}\left(E_p^*,E_d^*\right) = \frac{\hbar\,\ln(2)}{\Gamma(E_p^*,E_d^*)}. \tag{9}$$

Since we will eventually be interested in the ratio of the ambient temperature half-life to that at zero temperature, for the sake of simplicity, we assume that P_c remains the same for all levels and cancels in the ratio.

Once the half-lives dependent on excitation energies of the parent and daughter nuclei have been calculated, one can use the following expression [7] for the half-life of a nucleus at a given surrounding temperature T_s, namely,

$$t_{1/2}(T_s) = \left[\frac{1}{\mathcal{G}}\sum_{ij}\frac{g_{p_i}\exp\left(-E_{p_i}^*/(k_{\mathrm{B}}T_s)\right)}{t_{1/2}\left(E_{p_i}^*,E_{d_j}^*\right)}\right]^{-1}, \tag{10}$$

where $\mathcal{G} = \sum_i g_{p_i}\exp(-E_{p_i}^*/(k_{\mathrm{B}}T_s))$ is the standard partition function, and $g_{p_i} = (2J_{p_i}+1)$ is the statistical weight with J_{p_i} being the spin of the parent state p_i. The half-life $t_{1/2}\left(E_{p_i}^*,E_{d_j}^*\right)$ is calculated using (9).

Results for a few cluster decays are displayed in Fig. 2. The model predicts a sizeable decrease in cluster decay half-lives with increasing temperature. The present model can, in principle, be used to evaluate the temperature-dependent alpha decay rates too, and a simultaneous calculation of the two types of decay for the same parent nuclei will give us an idea of whether the role of cluster decay as compared to alpha decay changes at high temperatures.

3. Conclusions

Nuclear decay half-lives at finite ambient temperatures have been estimated in the present work with the objective of eventually including them in nucleosynthesis calculations of heavy elements. Alpha decay half-lives evaluated within a statistical approach using experimental data for the properties and half-lives of excited levels of nuclei display a strong dependence on the surrounding temperature. The corresponding sensitivity factor shows that the abundance of nuclei produced in r-process nucleosynthesis, which takes place at temperatures of the order of Giga Kelvins, can change even by two orders of magnitude. Motivated by these findings, a model for a similar calculation for light cluster decay is proposed, and predictions based on this model are presented. The inclusion of temperature-dependent half-lives in the r-process nucleosynthesis codes by formulating empirical formula to facilitate this inclusion for the decay rates of the hundreds of nuclei involved is planned for the future.

Acknowledgments

D.F.R-G. thanks the Faculty of Science, Universidad de Los Andes, Colombia, for financial support through Grant No. INV-2021-126-2314. O.L.C. acknowledges support from the National Science and Engineering Research Council (NSERC) and the Canadian Bureau for International Education.

References

[1] S. Hou, J. He, A. Parikh, D. Kahl, C. Bertulani, T. Kajino, G. Mathews, G. Zhao, *Astrophys. J.* **834**, 165 (2017).

[2] N. Council, *Connecting Quarks with the Cosmos: Eleven Science Questions for the New Century*, The National Academies Press, 2003.

[3] J. Cowan, F. Thielemann, J. Truran, *Phys. Rep.* **208**, 267 (1991).

[4] M. Arnould, S. Goriely, K. Takahashi, *Phys. Rep.* **450**, 97 (2007).

[5] J. Cowan, C. Sneden, J. Lawler, A. Aprahamian, M. Wiescher, K. Langanke, G. Martínez-Pinedo, F. Thielemann, *Rev. Mod. Phys.* **93**, 015002 (2021).

[6] C. Iliadis, *Nuclear Physics of Stars* John Wiley & Sons, 2007.

[7] R. Ward, W. Fowler, *Astrophys. J.* **238**, 266 (1980).

[8] J. Tuli, *National Nuclear Data Center wallet cards* Brookhaven National Laboratory, 2011.

[9] A. Soylu, C. Qi, *Nucl. Phys. A* **1013**, 122221 (2021).

[10] A. Sitenko, V. Tartakovskii, *Theory of Nucleus: Nuclear Structure and Nuclear Interaction* Springer, Dordrecht 1997.

[11] N.G. Kelkar, M. Nowakowski, *J. Phys. G* **43**, 105102 (2016).

[12] Z. Shand, SiRop, 2016.

[13] M. Kostka, N. Koning, Z. Shand, R. Ouyed, P. Jaikumar, *Astronomy Astrophys.* **568**, A97 (2014).

[14] M. Kostka, N. Koning, Z. Shand, R. Ouyed, P. Jaikumar, arXiv:1402.3824 (2014).

[15] Z. Shand, R. Ouyed, N. Koning, I. Dillmann, R. Krücken, P. Jaikumar, arXiv:1705.00099 (2017).

[16] A. Sandulescu, D. Poenaru, W. Greiner, *Sov. J. Part. Nucl.* **11**, 6 (1980).

[17] H. Rose, G. Jones, *Nature* **307**, 245 (1984).

[18] J. Perez Velasquez, N.G. Kelkar, N.J. Upadhyay, *Phys. Rev. C* **99**, 024308 (2019).

[19] D. Rojas-Gamboa, J. Velasquez, N.G. Kelkar, N. Upadhyay, *Phys. Rev. C* **105**, 034311 (2022).

[20] N. Fröman, P. Fröman, *JWKB Approximation* North-Holland, Amsterdam 1965.

[21] N.G. Kelkar, H. Casta neda, *Phys. Rev. C* **76**, 064605 (2007).

[22] D. Lang, K. Le Couteur, *Nucl. Phys.* **14**, 21 (1959).

[23] A. Antonov, J. Kanev, I. Petkov, M. Stoitsov, *Nuov. Cim. A* **101**, 525 (1989).

[24] R. Gupta, D. Singh, W. Greiner, *Phys. Rev. C* **75**, 024603 (2007).

[25] G. Satchler, W. Love, *Phys. Rep.* **55**, 183 (1979).

[26] R. Langer, *Phys. Rev.* **51**, 669 (1937).

[27] D. Rojas-Gamboa, N.G. Kelkar, O.L. Caballero, *Nucl. Phys. A* **1028**, 122524 (2022).